Combustion and Mixing Analysis of a Scramjet Combustor Using CFD

Pradeep Halder[1] Edla Franklin[2] Dr. P. Ravinder Reddy[3]
[1,2,3]Department of Mechanical Engineering
[1,2,3]CBIT, Hyderbad, Telangana state, India

Abstract— The present study is to determine flow field in the three-dimensional scramjet engine combustor with coupled implicit NS equations, the standard k-ε turbulence model are used and the finite-rate/eddy-dissipation reaction model has to be applied to simulate numerically for the flow field of the hydrogen, diesel and methane fueled scramjet combustor with a planer strut flame holder under two different working conditions, the working condition include the cold flow and engine ignition. ANSYS Fluent software is used to solve the analysis, with hot and cold inlet velocities, the mach number for air and fluids are 2 and 1 respectively, inflow fluids are varied as hydrogen, diesel and methane. Due to combustion the recirculation region behind the wedge becomes larger as compared to mixing case and it acts as a flame holder for the methane (CH4), hydrogen (H2) and diesel (C10H22) diffusion. It is also evident from the simulation studies; the combustion affects the flow field significantly. The leading edge shock reflected off the upper and lower combustor walls facilitates on setting of combustion when it hits the wake in a region where large portions of the injected fuel have been mixed up with the air. The pressure, velocity and temperature distributions along the geometry are estimated and discussed.

Key words: Combustion Efficiency, Diesel (C10H22), Methane (CH4), Hydrogen (H2), Shockwaves.

I. INTRODUCTION

The Supersonic Combustion Ramjet (SCRAMJET) engine has been recognized as the most promising air breathing propulsion system for the hypersonic flight (Mach number above 5) [1]. In recent years, the research and development of scramjet engine has promoted the study of combustion in supersonic flows. Extensive research is being carried out over the world for realizing the scramjet technology with hydrogen fuel with significant attention focused on new generations of space launchers and global fast-reaction reconnaissance missions. Mixing, ignition and flame holding in combustor, ground test facilities and numerical simulation of Scramjet engine are the critical challenges in the development of scramjet engine.

A. Mixing, Ignition and Flame Holding In A Scramjet Combustor

Among the critical components of the scramjet engine, the combustor presents the most formidable problems. The complex phenomenon of supersonic combustion involves turbulent mixing, shock interaction and heat release in supersonic flow [2]. The flow field within the combustor of scramjet engine is very complex and poses a considerable challenge in design and development of a supersonic combustor with an optimized geometry. Such combustor shall promote sufficient mixing of the fuel and air so that the desired chemical reaction and thus heat release can occur within the residence time of the fuel -air mixture. In order to accomplish this task, it requires a clear understanding of fuel injection processes and thorough knowledge of the processes governing supersonic mixing and combustion as well as the factors, which affects the losses within the combustor.

The designer shall keep in mind the following goals namely,

- Good and rapid fuel air mixing
- Minimization of total pressure loss
- High combustion efficiency

II. OBJECTIVE

This work is carried out on scramjet engine with 3 fluids. To model the flow inside the Scramjet engine using the Computational Fluid Dynamics (CFD) program and the combustor geometry of the Scramjet engine for maximum thrust at a single operating condition (Mach number). The configuration of the Scramjet was varied by three fluid parameters. Shigeru Aso et.al [3] worked on the topic of "Fundamental study of supersonic combustion in pure air flow with use of shock tunnel", and their findings are – The increase of injection pressure generated strong bow shock, resulting in the pressure loses. The shock generator is an effective method to accelerate the combustion. The increase of the injection total pressure raises the penetration of fuel; thus, the reaction zone expands to the center of flow field. K. M. Pandey and Siva Sakthivel. T [4] worked on the topic of "Recent Advances in Scramjet Fuel Injection - A Review", and their findings are – Fuel injection techniques into scramjet engines are a field that is still developing today. The fuel that is used by scramjets is usually either a liquid or a gas.

The fuel and air need to be mixed to approximately stoichiometric proportions for efficient combustion to take place. The main problem of scramjet fuel injection is that the airflow is quite fast, meaning that there is minimal time for the fuel to mix with the air and ignite to produce thrust (essentially milliseconds).Hydrogen is the main fuel used for combustion [5]. Hydrocarbons present more of a challenge compared to hydrogen due to the longer ignition delay and the requirement for more advanced mixing techniques. Enhancing the mixing, and thus reducing the combustor length, is an important aspect in designing scramjet engines. There are number of techniques used today for fuel injection into scramjet engines.

III. EQUATION

A. Continuity Equations

The basic continuity equation of fluid flow is as follows:
Net flow out of control volume = time rate of decrease of mass inside control volume

The continuity equation in partial differential equation form is given by,

$$\delta\rho/\delta t + \nabla.(\rho V) = 0 \qquad 3.1$$

ρ = Fluid density

$\delta\rho/\delta t$ = the rate of increase of density in the control volume.

∇. (ρV)=the rate of mass flux passing out of control volume.

The first term in this equation represents the rate of increase of density in the control volume and the second term represents the rate of mass flux passing out of the control surface, which surrounds the control volume. This equation is based on Eulerian approach. In this approach, a fixed control volume is defined and the changes in the fluid are recorded as the fluid passes through the control volume. In the alternative Lagrangian approach, an observer moving with the fluid element records the changes in the properties of the fluid element. Eulerian approach is more commonly used in fluid mechanics [6]. For a Cartesian coordinate system, where u, v, w represent the x, y, z components of the velocity vector, the continuity equation becomes

$$\frac{\partial \rho}{\partial t}+\frac{\partial}{\partial x}(\rho u)+\frac{\partial}{\partial y}(\rho v)+\frac{\partial}{\partial z}(\rho w)=0 \qquad 3.2$$

A flow in which the density of fluid assumed to remain constant is called Incompressible flow.

For Incompressible flow, ρ =Constant.

B. Momentum Equation

Newton's Second Law applied to a fluid passing through an infinitesimal, fixed control volume yields the following momentum equation:

$$\frac{\partial}{\partial t}(\rho v)+\nabla .\rho VV = \rho f + \nabla .\tau_{ij} \qquad 3.3$$

Where, δ/δt(ρv)→ represents rate of increase of momentum per unit volume.

∇ρ V → represents the rate of momentum lost by convection through the control volume surface.

ρ f → represents the body force per unit volume.

∇. π_{ij}→ represents the surface force per unit volume and π_{ij} →stress tensor.

This equation is good approximation for incompressible flow of a gas.

C. Theory

Solutions in CFD are obtained by numerically solving a number of balances over a large number of control volumes or elements. The numerical solution is obtained by supplying boundary conditions to the model boundaries and iteration of an initially guessed solution. The balances, dealing with fluid flow, are based on the Navier Stokes Equations for conservation of mass (continuity) and momentum. These equations are modified per case to solve a specific problem. The control volumes (or) elements, the mesh are designed to fill a large scale geometry, described in a CAD file. The density of these elements in the overall geometry is determined by the user and affects the final solution. Too coarse a mesh will result in an over simplified flow profile, possibly obscuring essential flow characteristics [7]. Too fine meshes will unnecessarily increasing iteration time. After boundary conditions are set on the large scale geometry the CFD code will iterate the entire mesh using the balances and the boundary conditions to find a converging numerical solution for the specific case.

D. The General Differential Equation

A generalized conservation principle is obeyed by all the independent variables of interest, so the basic balance or conservation equation is (Outflow from cell) – (inflow into the cell) = (net source within the cell.)

The quantities being balanced are the dependent variables like mass of a phase, mass of a chemical species, energy, momentum, turbulence quantities, electric charge etc. The terms appearing in the balance equation are convection, diffusion, time variation and source terms. If the dependent variable is denoted byϕ, the general differential equation or the general purpose CFD equation is given as

$$\delta(\beta\phi)/\delta t \ +\mathrm{div}(\beta u\phi-\Gamma \mathrm{grad}\ \phi) = S+S_{BC} \qquad 3.4$$

Where, p, u, v, w, h, k, £ =Dependent variable, (ϕ) t, x, y, z =Independent variable Γ=Exchange coefficient β=Scalars S =source terms S_{BC} = Boundary conditions sources

Div =divergence (V. J) Grad =gradient (Vϕ)

E. Reynolds Averaged Navier-Stokes Equation

In the conventional averaging procedure, following Reynolds, we define a time averaged quantity f as fluctuations in other fluid properties such as viscosity, thermal conductivity, and specific heat are usually small and will be neglected here.

By definition, the average of a fluctuating quantity is zero

$$\bar{f}' = \frac{1}{\Delta t}\int_{t_0}^{t_0+\Delta t} f'dt = 0 \qquad 3.5$$

It should be clear from these definitions that for symbolic flow variable f and g, the following relations hold:

$$\overline{fg'}=0 \qquad \overline{f+g}=\bar{f}+\bar{g} \qquad 3.6$$

F. Reynolds Form of Continuity Equation

Reynolds form of the momentum equation for incompressible flow is

$$\frac{\partial}{\partial t}(\rho\overline{u_i})+\frac{\partial}{\partial t}\left(\rho\overline{u_i u_j}\right)=-\frac{\partial \bar{p}}{\partial x_i}+\frac{\partial}{\partial x_j}\left(\overline{\tau_{ij}}-\overline{\rho u_i' u_j'}\right) \qquad 3.7$$

For compressible flows the momentum equation becomes

$$\partial\rho/\partial t + \partial/\partial x_j(\rho\ u_j) = 0 \qquad 3.8$$

$$-\overline{\rho u_i' u_j'} = \mu_T\left(\frac{\partial u_i}{\partial x_j}+\frac{\partial u_j}{\partial x_i}\right)-\frac{2}{3}\delta_{ij}\left(\mu_T\frac{\partial u_k}{\partial x_k}+\rho\bar{k}\right) \qquad 3.9$$

Where μ_T the turbulent viscosity, k is is the kinetic energy of turbulence given by,

$$\bar{k} \quad \frac{\overline{u_i' u_i'}}{2} \qquad 3.10$$

By analogy with kinetic theory, by which molecular (laminar) viscosity for gases be evaluated with reasonable accuracy, we might expect that the turbulent viscosity can be modeled as

$$\mu_T = \rho v_T l \qquad 3.11$$

Where V_T and l are characteristic velocity and length scale of turbulence respectively. The problem is to find suitable means of evaluating them.

Algebraic turbulence models invariably utilize Boussinesq assumption. One of the most successful of this type of model was suggested by Prandtl and is known as "mixing length hypothesis".

$$\mu_T = \rho l^2 \left|\frac{\partial u}{\partial y}\right| \quad 3.12$$

Where a mixing length can be thought of as a transverse distance over which particles maintain their original momentum, somewhat on the order of a mean free path for the collision or mixing of globules of fluid. The product can be interpreted as the characteristic velocity of turbulence, VT. In the above equation, u is the component of velocity in the primary flow direction, and y is the coordinate transverse to the primary flow direction.

There are other models, which use one partial differential equation for the transport of turbulent kinetic energy (TKE) from which velocity scales are obtained. The length scale is prescribed by an algebraic formulation.

The most common turbulence model generally used is the two-equation turbulence model or k-Є model. There are so many variants of this model. In these models the length scale is also obtained from solving a partial differential equation.

The most commonly used variable for obtaining the length scale is dissipation rate of turbulent kinetic energy denoted by E. Generally the turbulent kinetic energy is expressed as turbulent intensity σ as defined below.

K= (Actual K.E in Flow) – (mean K.E in Flow)

$$k = 1/2\left(u'^2 + v'^2 + w'^2\right) \qquad \sigma = \frac{1}{U'}\left(\frac{u'^2 + v'^2 + w'^2}{3}\right)^{1/2}$$

$$\mu_t = C_\mu \rho \overline{k^2}/\varepsilon \quad 3.13,\ 3.14$$

The transport PDE used in standard k-ε model is as follows

$$\rho\frac{D\bar{k}}{Dt} = \frac{\partial}{\partial x_j}\left[(\mu + \mu_T/\mathrm{Pr}_k)\frac{\partial \bar{k}}{\partial x_j}\right] + \left[\mu_T\left(\frac{\partial u_i}{\partial x_j} + \frac{\partial u_j}{\partial x_i}\right) - \frac{2}{3}\rho\bar{k}\delta_{ij}\right]\frac{\partial u_i}{\partial x_j} - \rho\varepsilon \quad 3.15$$

Thus for any turbulent flow problem, we have to solve in addition to continuity, momentum and energy equations, two equations for transport of TKE and its dissipation rate.

$$\rho\frac{D\varepsilon}{Dt} = \frac{\partial}{\partial x_j}\left[(\mu + \mu_T/\mathrm{Pr}_\varepsilon)\frac{\partial \varepsilon}{\partial x_j}\right] + C_{\varepsilon_1}\frac{\varepsilon}{k}\left[\mu_T\left(\frac{\partial u_i}{\partial x_j} + \frac{\partial u_j}{\partial x_i}\right) - \frac{2}{3}\rho\bar{k}\delta_{ij}\right]\frac{\partial u_i}{\partial x_j} - C_{\varepsilon_2}\rho\frac{\varepsilon^2}{k} \quad 3.16$$

G. Turbulence Modeling

Special attention needs to be paid to accurate modeling of turbulence. The presence of turbulent fluctuations, which are functions of time and position, contribute a mean momentum flux or Reynolds stress for which analytical solutions are nonexistent. These Reynolds stresses govern the transport of momentum due to turbulence and are described by additional terms in the Reynolds-averaged Navier-Stokes equations. The purpose of a turbulence model is to provide numerical values for the Reynolds stresses at each point in the flow. The objective is to represent the Reynolds stresses as realistically as possible, while maintaining a low level of complexity. The turbulence model chosen should be best suited to the particular flow problem.

These often help in understanding complex flow phenomena that are sometimes difficult to see from static plots.

$$\frac{\partial}{\partial t}\int_\Omega U d\Omega + \int_S \overline{F}\, d\overline{S} = \int_\Omega Q d\Omega \quad 3.17$$

Ω- Control volume S- Surface enveloping Ω U- Conserved scalar F- Diffusive and convective flux
Q- Volumetric source of U

H. Modeling and Meshing of Scramjet Combustor

In the present analysis the DLR scramjet combustor with strut injection dimension is selected for simulation. A schematic of the DLR scramjet is presented in Fig.1. Preheated air is expanded through a Laval nozzle and enters the combustor section at Ma = 2.0. The combustor has a width of 40 mm and a height of 50 mm at the entrance and a divergence angle of the upper channel wall of three degrees to compensate for the expansion of the boundary layer. A planer wedge shaped strut is placed in the combustion chamber downstream of the nozzle. Just downstream of the nozzle the height of the 32 mm long strut is 0.295 mm. along the first 100 mm downstream of the nozzle, the side walls and the upper wall are made from quartz glass to allow optical access and to minimize the reflection of scattered light on the wall opposite the observation window. Hydrogen (H_2) is injected at Ma =1.0 through a planer strut injector with diameter of 0.295 mm, in the strut base. Typical mass flows in the experiments [8] were varied between 1.0 and 1.5 kg/s for the air and between 1.5 and 4.0 g/s for H_2, which correspond to equivalence ratios between 0.034 and 0.136, respectively. The hydrogen is injected at ambient temperature and pressure, i.e. at T = 250 K and p =105 Pa, whereas the air was injected at T = 340 K and p =105 Pa.

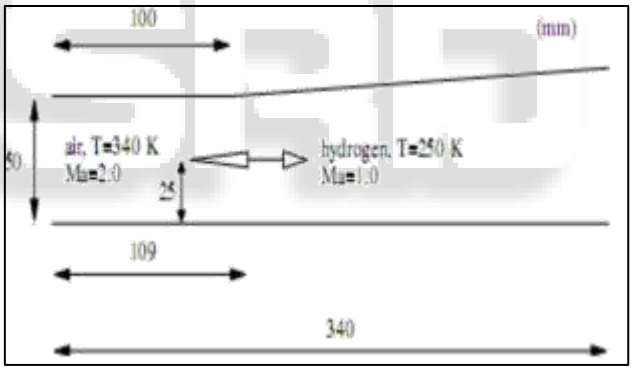

Fig. 1: Schematic of the supersonic combustion chamber

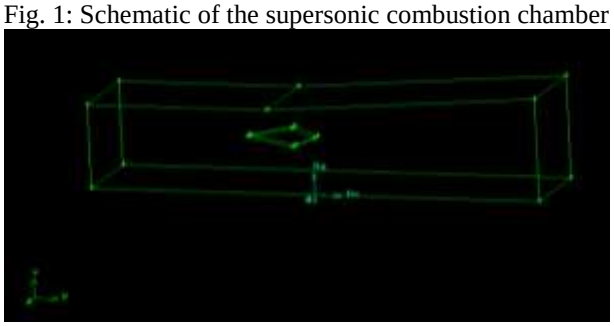

Fig. 2: Scramjet combustor

The Fig.2 shows the scramjet wireframe model which is created using Gambit as per the dimensions of Fig.1. The Fig.3 shows the meshing of strut which is done using tria 2d-elements with 0.1mm element size in Gambit. Fig.4 shows the meshing of boundary and scramjet combustor which is done using tetrahedron elements and the model consist of 99318 faces, 48059 cells and 9690 nodes using Gambit.

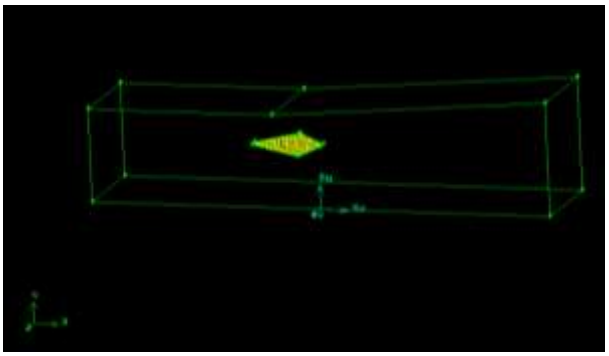

Fig. 3: Meshing scramjet combustor with sturdy

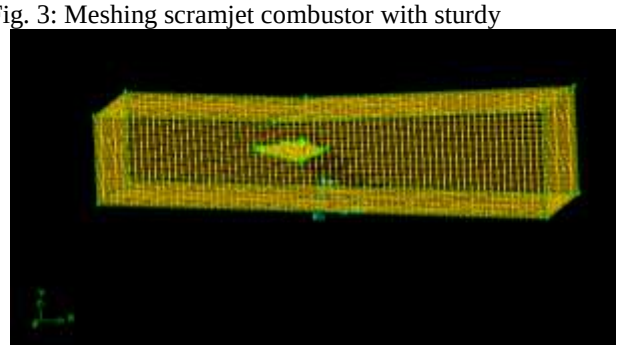

Fig 4: Meshing of boundary and scramjet combustor

IV. RESULTS AND DISCUSSIONS

Due to combustion the recirculation region behind the wedge becomes larger as compared to mixing case and it acts as a flame holder for the methane (CH_4), hydrogen (H_2) and diesel ($C_{10}H_{22}$) diffusion flame. It is also evident from the Fig. 6, 13 and 16 , the combustion affects the flow field significantly. The leading edge shock reflected off the upper and lower combustor walls facilitates the on setting of combustion when it hits the wake in a region where large portions of the injected fuel have been mixed up with the air. After its first encounter with the flame the leading edge shock is drastically weakened and the characteristic shock wave pattern of the cold flow cases is almost gone.

A. Contours Of Methane(Ch_4)- Air

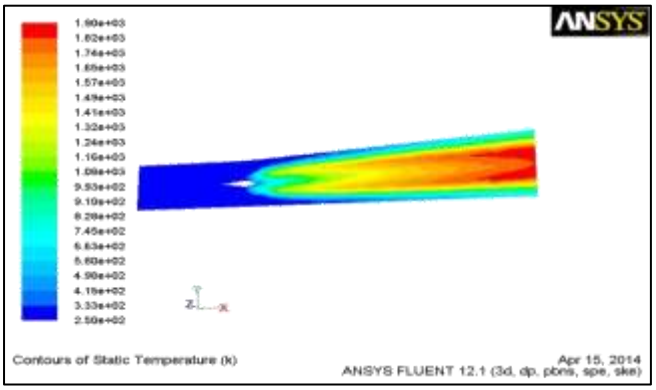

Fig. 5: Variation of static temperature of ch_4 in scramjet

The static temperature variation in the combustor given in Fig.5, it shows that the temperature is constant up to x=109mm, after that it is increasing gradually to maximum of 1.9e3 K at the point of x=245mm. The temperature variation in the top and bottom side of the combustion chamber, at the top wall maximum temperature is 5.80e2 K at the bottom side it is maximum of 4.98e2 K.

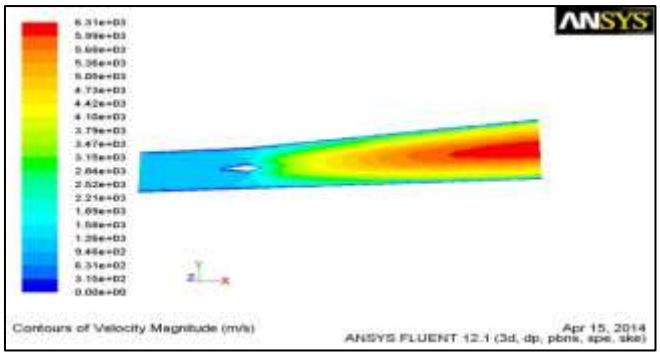

Fig. 6: Variation of velocity magnitude of ch_4 in scramjet

The Fig.6 is giving the details about how the velocity variation is taking place inside the Combustion chamber, air is entering at Mach number 2 it is constant up to x = 77mm after that it is started Decreasing to 0.3 it happened due to Shape of the Strut, this subsonic region acting as flame holder for combustion. After some distances speed of the flame become Supersonic

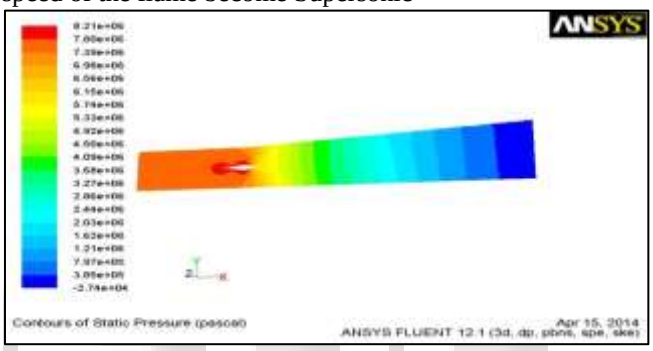

Fig. 7: Variation of static pressure of ch_4 in scramjet

The static pressure variation in the combustor shown in Fig 7. From the Figure it is clear that at the entrance up to x= 77 mm static pressure is 8.21e6 bar, it is decreased to 4.50e6 bar at the centre of the combustor, it is due to reflection of shockwaves after some distances it came to 2.44e6 bar, shows the variation of pressure in the top and bottom side of the combustion chamber, it is clear that up to the distance of 0.77m the pressure is constant, after that it is decreased to 1.21e6 bar in bottom wall and 3.85e5 bar in top wall.

B. Contours Of Hydrogen (H2)-Air

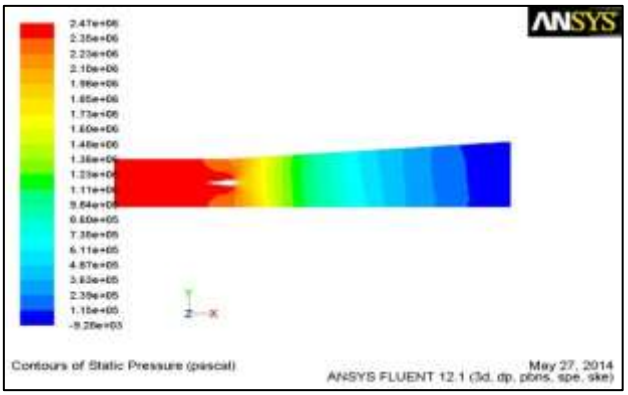

Fig. 8: Variation of static pressure of H_2 in scramjet

The Fig.8 static pressure variation in the combustor. From the Figure it is clear that at the entrance up to x= 77 mm static pressure is 2.47e6 bar, it is decreased to 1.36e6 bar at the centre of the combustor, it is due to reflection of shockwaves after some distances it came to

8.6e5 bar, shows the variation of pressure in the top and bottom side of the combustion chamber, it is clear that up to the distance of 0.77m the pressure is constant, after that it is decreased to 1.15e5 bar in bottom wall and 2.39e5 bar in top wall.

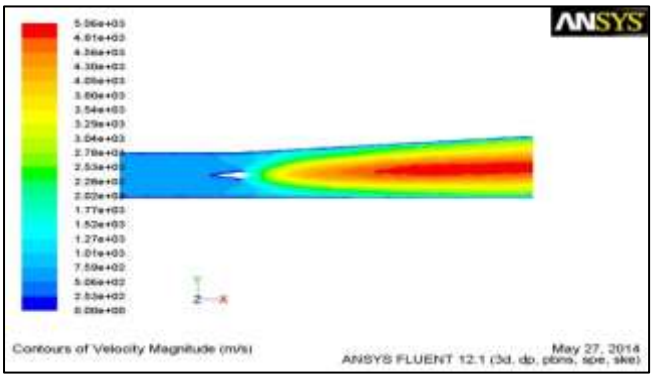

Fig. 9: Variation of velocity magnitude of H_2 in scramjet

The Fig.9 is giving the details about how the velocity variation is taking place inside the Combustion chamber, air is entering at Mach number 2 it is constant up to x = 77mm after that it is started decreasing to 0.4 it happened due to Shape of the Strut, this subsonic region acting as flame holder for combustion. After some distances speed of the flame become Supersonic.

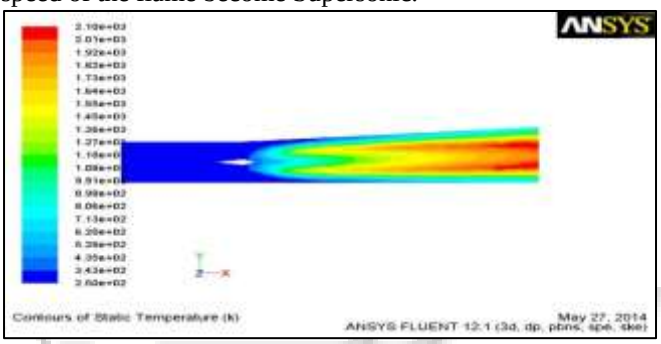

Fig.10: Variation of static temperature of H_2 in scramjet

The static temperature variation in the combustor given in Fig.10, it shows that the temperature is constant up to X = 109mm, after that it is increasing gradually to maximum of 2.10e3 K at the point of x=245mm. The temperature variation in the top and bottom side of the combustion chamber, at the top wall maximum temperature is 8.06e2 K at the bottom side it is maximum of 7.13e2 K.

C. Contours of Diesel ($C_{10}h_{22}$)-Air

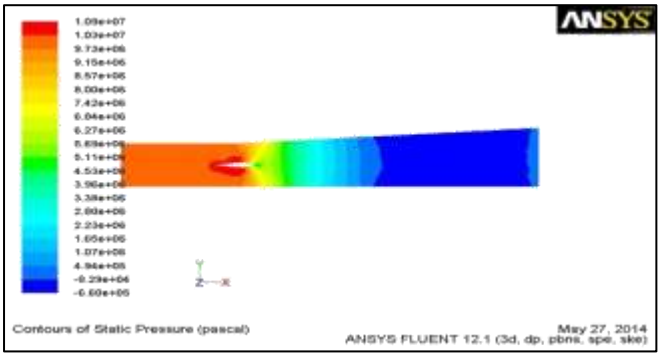

Fig. 11: Variation of static pressure of diesel ($C_{10}H_{22}$)-air in scramjet

The static pressure variation in the combustor shown in Fig.11. From the Figure it is clear that at the entrance up to x= 77 mm static pressure is 1.09e6 bar, it is decreased to 5.11e6 bar at the centre of the combustor, it is due to reflection of shockwaves after some distances it came to 28 bar, shows the variation of pressure in the top and bottom side of the combustion chamber, it is clear that up to the distance of 0.77m the pressure is constant, after that it is decreased to 1.07e6 bar in bottom wall and 4.94e5 bar in top wall.

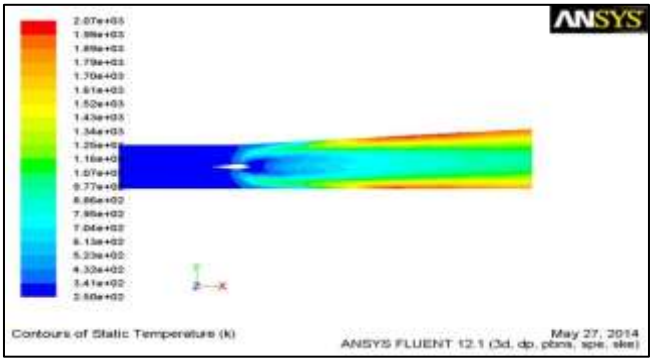

Fig. 12: Variation of static temperature of diesel ($C_{10}H_{22}$)-air in scramjet

The Fig.12 shows the static temperature variation in the combustor, it shows that the temperature is constant up to X = 109mm, after that it is increasing gradually to maximum of 2.07e2 K at the point of x=245mm. The temperature variation in the top and bottom side of the combustion chamber, at the top wall maximum temperature is 7.94e2 K at the bottom side it is maximum of 7.94e2 K.

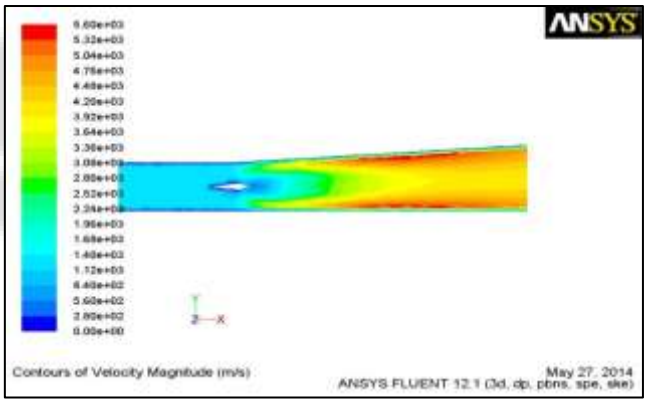

Fig. 13: Variation of velocity magnitude of diesel ($C_{10}H_{22}$)-air in scramjet

The Fig.13 is giving the details about how the velocity variation is taking place inside the Combustion chamber, air is entering at Mach number 2 it is constant up to x = 77mm after that it is started decreasing to 0.45 it happened due to Shape of the Strut, this subsonic region acting as flame holder for combustion. After some distances speed of the flame become Supersonic.

Condition	Static pressure, Pa	Velocity, m/s	Temperature, K
Methane CH_4	8.21e6	6.31e3	1.90e3
Diesel, $C_{10}H_{22}$	1.09e7	5.60e3	2.07e3
Hydrogen, H_2	2.47e6	5.06e3	2.10e3

Table1: Variation of pressure, velocity and temperature

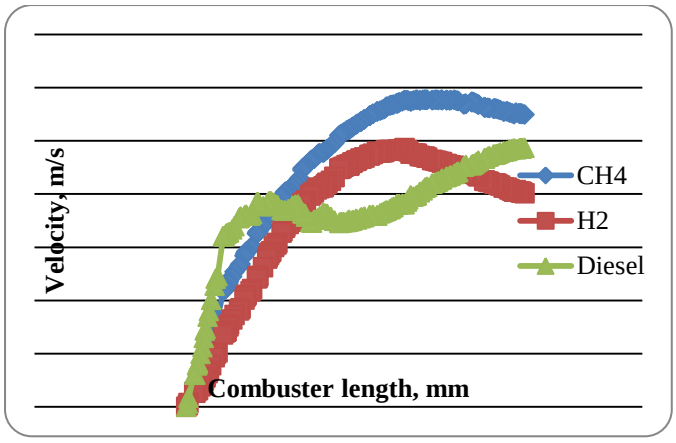

Fig. 14: comparision of velocity with respect to combuster length

Fig.14 shows the variation of velocity with respeect to the combuster distance. For comparing three fluids methane, diesel and hydrogen, velocity at the centre of the combuster is maximum in methane and diesel fluids, in hydrogen velocity is decreased.

The primary hydrogen fuel for scramjets is the bi-hydrogen molecule in a liquid state. Hydrogen fuelled scramjets have been the most popular thus far. The selection of hydrogen fuel is based on several important advantages that it provides over other potential scramjet fuels. Primarily, hydrogen burns rapidly and produces high quantities of energy. Rapid burning reduces ignition delay and permits satisfactory combustion at high airflow velocities. hydrogen fuelled scramjets produce a higher specific impulse (pounds of thrust produced per pound of fuel burnt) than other-fuelled systems.

Hydrogen is a gas at ambient temperatures. Even though it is usually stored in a liquid state, it vaporises immediately upon release into the air stream without the need for an injector spray. This reduces ignition delay and results in easier mixing with the airstream. Conversely, liquid hydrocarbon fuels are sprayed into the chamber as droplets, which must evaporate before combustion can occur.

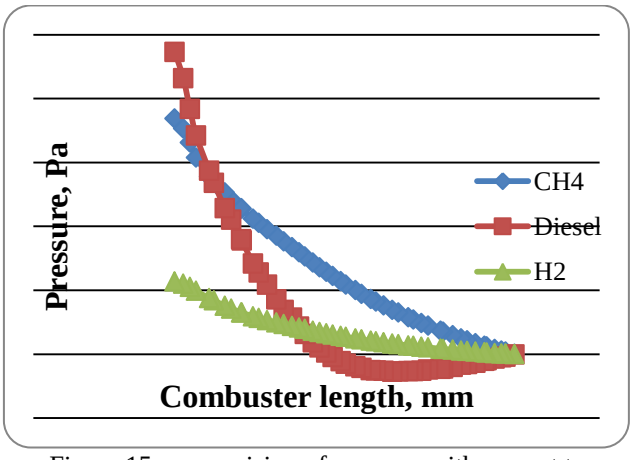

Figure 15: comparision of pressure with respect to combuster length

Fig.15 shows the variation of pressure with respeect to the combuster distance. For comparing three fluids methane, diesel and hydrogen, pressure at the centre of the combuster is sudden decrease in methane and diesel fluids, in hydrogen combuster is pressure is gradually decreased.

The combustion process in the scramjet engine is dependent on the ambient pressure. This lead to a highly parabolic trajectory with a near vertical decent and ensured a correlation could be developed over an envelope of ambient pressures.

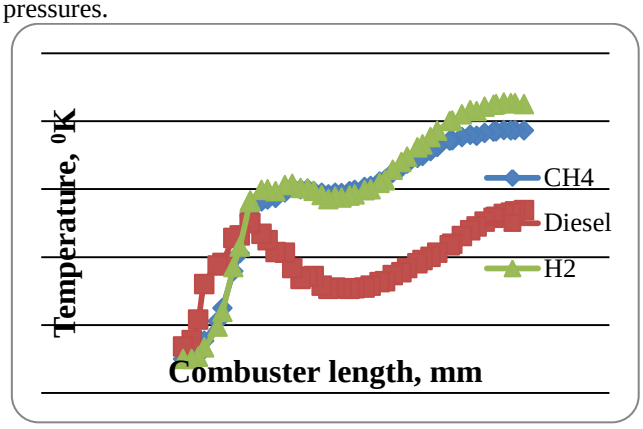

Figure 16: comparision of temperature with respect to combuster length

Fig.16 shows the variation of temperature with respect to the combuster distance. For comparing three fluids methane, diesel and hydrogen, Hydrogen fuelled combuster temperature is maximum at the outlet compare to methane and diesel fuelled scramjets.

The sudden increase in pressure and temperature in the engine can lead to the combustion chamber exploding.

V. CONCLUSIONS

The numerical method employed in this work can be used to accurately investigate the flow field of the scramjet combustor with planer strut flame holder, and capture the shock wave system reasonably. In order to investigate the flame holding mechanism of the planer strut in supersonic flow, the standard k-ε turbulence model is introduced to simulate the flow field of the hydrogen fueled, CH_4 and Diesel fuel scramjet combustor with a strut flame holder. The maximum static pressure, maximum velocity, and maximum temperature in the scramjet combustor with planer strut flame holder for Methane CH_4 is 8.21 e6 Pa, 6.31e3 m/s and 1900 ^{0}K respectively. The maximum static pressure, maximum velocity, and maximum temperature in the scramjet combustor with planer strut flame holder for Diesel, $C_{10}H_{22}$ is 1.09 e7 Pa, 5.60e3 m/s and 2070 ^{0}K respectively. The maximum static pressure, maximum velocity, and maximum temperature in the scramjet combustor with planer strut flame holder for Hydrogen, H_2 is 2.47 e6 Pa5.06e3 m/s and 2100 ^{0}K respectively.

REFERENCES

[1] Glawe, M. Samimiy, A. Nejad, T. Cheng, Effects of nozzle geometry on parallel injection from base of an extended strut into supersonic flow, AIAA paper 95-0522, 1995.

[2] D. Papamoschou, Analysis of partially mixed supersonic ejector, Journal of Propulsion and Power 12 (1996) 736–741.

[3] Shigeru Aso, ArifNur Hakim, Shingo Miyamoto, Kei Inoue and Yasuhiro Tani, "Fundamental study of

supersonic combustion in pure air flow with use of shock tunnel", Department of Aeronautics and Astronautics, Kyushu University, Japan , Acta Astronautica, vol 57, 2005, pp.384 – 389.

[4] K. M. Pandey and T.Sivasakthivel, "Recent Advances in Scramjet Fuel Injection - A Review," International Journal of Chemical Engineering and Applications vol. 1, no. 4, pp. 294-301, 2010.

[5] T. Mitani, T. Kouchi, Flame structures and combustion efficiency computed for a Mach 6 scramjet engine, Combustion and Flame 142 (2005) 187–196.

[6] I. Waitz, F. Marble, E. Zukoski, Investigation of a contoured wall injector for hypervelocity mixing augmentation, AIAA Journal 31 1993) 1014–1021.

[7] D. Riggins, Thrust losses in hypersonic engines, part 2: Applications, Journal of Propulsion and Power 13 (1997) 288–295.

[8] CFD Analysis of Mixing and Combustion of a Scramjet Combustor with a Planer Strut injector.

